Kinetic Investigation of Homogeneous H_2-D_2 Equilibration Catalyzed by Pt−Au Cluster Compounds. Characterization of the Cluster $[(H)Pt(AuPPh_3)_9](NO_3)_2$

Leon I. Rubinstein and Louis H. Pignolet*

Department of Chemistry, University of Minnesota, Minneapolis, Minnesota 55455

Received November 29, 1995[⊗]

The new Pt−Au hydrido cluster compound $[(H)Pt(AuPPh_3)_9](NO_3)_2$ (**3**) has been synthesized and characterized by NMR, FABMS, and single-crystal X-ray diffraction [triclinic, $P\bar{1}$, $a = 17.0452(1)$ Å, $b = 17.4045(2)$ Å, $c = 55.2353(1)$ Å, $\alpha = 89.891(1)°$, $\beta = 85.287(1)°$, $\gamma = 75.173(1)°$, $V = 15784.0(2)$ Å^3, $Z = 4$ (two molecules in asymmetric unit), residual $R = 0.089$ for 45 929 observed reflections and 3367 variables, Mo Kα radiation]. The $Pt(AuP)_9$ core geometry is a distorted icosahedron with three vertices vacant. The Pt−Au, Au−Au, and Au−P distances are within the normal ranges observed in other Pt−Au clusters. This cluster is a catalyst for H_2-D_2 equilibration in homogeneous solution phase and has been used in a general mechanistic study of this reaction catalyzed by Pt−Au clusters. We previously proposed that a key step in the mechanism for catalytic H_2-D_2 equilibration is the dissociation of a PPh_3 ligand to give a cluster with an open Au site for bonding of H_2 or D_2. This was based on qualitative observations that PPh_3 inhibited the rate of HD production with $[Pt(AuPPh_3)_8](NO_3)_2$ (**1**) as catalyst. In order to test this hypothesis, phosphine inhibition (on the rate of HD production) and phosphine ligand exchange kinetic experiments were carried out with $[(H)(PPh_3)Pt(AuPPh_3)_7](NO_3)_2$ (**2**) and **3**. In this paper we show that the rate constant for phosphine dissociation determined from the PPh_3 inhibition rate study of H_2-D_2 equilibration with cluster **2** is nearly identical to the rate constant for dissociative phosphine ligand exchange. The slower rate for H_2-D_2 equilibration observed with **3** compared with **2** (5.5×10^{-3} *vs* 7.7×10^{-2} turnover s^{-1}) is explained by its smaller rate constant for phosphine dissociation (2.8×10^{-5} *vs* 2.9×10^{-4} s^{-1}). The fact that clusters **2** and **3** show similar kinetic behaviors suggests that the PPh_3 dissociation step in the catalytic H_2-D_2 equilibration is general for 18-electron hydrido Pt−$AuPPh_3$ clusters.

Introduction

A large number of phosphine-stabilized Pt−Au cluster compounds have been prepared and characterized during the past decade.[1−8] The most extensively studied cluster of this type is $[Pt(AuPPh_3)_8](NO_3)_2$ (**1**).[1,3] This Pt-centered cluster has 16 valence electrons, $(S^\sigma)^2(P^\sigma)^4$, in its metal frame according to the electron-counting formalism for M-centered, high-nuclearity clusters advanced by Mingos.[2,9] Cluster **1** reacts with 2-electron-donor substrates L, for example CO and RNC, to give 18-electron, $(S^\sigma)^2(P^\sigma)^6$, adducts $[(L)Pt(AuPPh_3)_8](NO_3)_2$.[1,3] The recent discovery that **1** reacts with molecular hydrogen[10,11] led to the preparation of many new hydrido clusters such as $[(H)_2Pt(AuPPh_3)_8](NO_3)_2$,[10,11] $[(H)Pt(AuPPh_3)_8]NO_3$,[6,12] $[(H)Pt(AuPPh_3)_8(AgNO_3)]NO_3$,[6] and $[(H)Pt(AuPPh_3)_8(CuCl)_2]NO_3$.[7] This discovery also led in the study of Pt−Au clusters as hydrogen activation catalysts. $[Pt(AuPPh_3)_8](NO_3)_2$ (**1**) and related clusters are excellent catalysts for H_2-D_2 equilibration ($H_2 + D_2 \rightleftarrows 2HD$) in homogeneous solution phase and in the solid state.[10,11,13] They were also found to catalyze $D_2(g)-H_2O(l)$ isotope exchange in homogeneous pyridine solution.[12] These catalysis reactions have proven useful as probes of structure−reactivity relations for a number of heterometallic clusters.[13] The H_2-D_2 equilibration reaction has also been useful to probe the nature of Pt−Au clusters on silica and alumina supports.[14] Considerable effort is being devoted to studying the mechanism of these H_2 activation reactions. Hydrogen activation is of fundamental importance in the area of catalysis, and very few studies have been carried out with heterometallic cluster compounds. These novel compounds are providing an excellent opportunity to study the details of H_2 activation by heterometallic clusters.

Catalytic H_2-D_2 equilibration in homogeneous solution was extensively studied for **1** by a combination of kinetic and NMR measurements.[13] The mechanism shown in eq I was proposed

$$M \underset{-(H,D)_2}{\overset{+(H,D)_2}{\rightleftharpoons}} M(H,D)_2 \underset{+PPh_3}{\overset{-PPh_3}{\rightleftharpoons}} M^*(H,D)_2 \underset{-(H,D)_2}{\overset{+(H,D)_2}{\rightleftharpoons}} M^*(H,D)_4 \quad \text{(I)}$$

for the catalytic production of HD. Here, M refers to $[Pt(AuPPh_3)_8](NO_3)_2$, M* refers to M with one less PPh_3 ligand,

[⊗] Abstract published in *Advance ACS Abstracts,* November 1, 1996.

(1) Pignolet, L. H.; Aubart, M. A.; Craighead, L. K.; Gould, R. A. T.; Krogstad, D. A.; Wiley, J. S. *Coord. Chem. Rev.* **1995**, *143*, 219.
(2) Mingos, D. M. P.; Watson, M. J. *Adv. Inorg. Chem.* **1992**, *39*, 327.
(3) Steggerda, J. J. *Comments Inorg. Chem.* **1991**, *11*, 113.
(4) Mueting, A. M.; Bos, W.; Alexander, B. D.; Boyle, P. D.; Casalnuovo, J. A.; Balaban, L. N.; Ito, L. N.; Johnson, S. M.; Pignolet, L. H. *New J. Chem.* **1988**, *12*, 505.
(5) Teo, B. K.; Zhang, H.; Shi, X. *J. Am. Chem. Soc.* **1993**, *115*, 8489.
(6) Kappen, T. G. M. M.; Schlebos, P. P. J.; Bour, J. J.; Bosman, W. P.; Beurskens, G.; Smits, J. M. M.; Beurskens, P. T.; Steggerda, J. J. *Inorg. Chem.* **1995**, *34*, 2121.
(7) Kappen, T. G. M. M.; Schlebos, P. P. J.; Bour, J. J.; Bosman, W. P.; Smits, J. M. M.; Beurskens, P. T.; Steggerda, J. J. *Inorg. Chem.* **1995**, *34*, 2133.
(8) Gould, R. A. T.; Craighead, K. L.; Wiley, J. S.; Pignolet, L. H. *Inorg. Chem.* **1995**, *34*, 2902.
(9) Mingos, D. M. P.; Wales, D. J. *Introduction to Cluster Chemistry*; Prentice Hall: Englewood Cliffs, NJ, 1990. Mingos, D. M. P.; Johnson, R. L. *Struct. Bonding* **1987**, *68*, 29. Stone, A. J. *Inorg. Chem.* **1981**, *20*, 563.
(10) Aubart, M. A.; Pignolet, L. H. *J. Am. Chem. Soc.* **1992**, *114*, 7901.
(11) Kappen, T. G. M. M.; Bour, J. J.; Schlebos, P. P. J.; Roelofsen, A. M.; Van der Linden, J. G. M.; Steggerda, J. J.; Aubart, M. A.; Krogstad, D. A.; Schoondergang, M. F. J.; Pignolet, L. H. *Inorg. Chem.* **1993**, *32*, 1074.
(12) Aubart, M. A.; Koch, J. F. D.; Pignolet, L. H. *Inorg. Chem.* **1994**, *33*, 3849.
(13) Aubart, M. A.; Chandler, B. D.; Gould, R. A. T.; Krogstad, D. A.; Schoondergang, M. F. J.; Pignolet, L. H. *Inorg. Chem.* **1994**, *33*, 3724.
(14) Graf, I. V. G.; Bacon, J. W.; Consugar, M. B.; Curley, M. E.; Ito, L. N.; Pignolet, L. H. *Inorg. Chem.* **1996**, *35*, 689.

S0020-1669(95)01516-3 CCC: $12.00

and $(H,D)_2$ refers to the three isotopic possibilities H_2, D_2, and HD. The first step of this mechanism was directly observed by ^1H and ^{31}P NMR and is not rate limiting. Step 2 was implicated by the inhibition in the rate of HD production by added PPh_3 ligand, but a quantitative kinetic analysis was not possible because of cluster instability in the presence of H_2 and PPh_3. A key feature of this mechanism is the formation of the $M^*(H,D)_4$ species. It was suggested that the open Au site was necessary to bind the incoming D_2 ligand, thus avoiding a 20-electron intermediate.[8,13] This species would rapidly scramble H and D, producing HD by a back-elimination reaction as shown in eq I. Because very little is known about the reversible reaction of H_2 with metal cluster compounds, it was considered important to further study the mechanism of this H_2-D_2 equilibration catalysis. In this paper we report the quantitative study of PPh_3 inhibition of the kinetics of H_2-D_2 equilibration for $[(H)(PPh_3)Pt(AuPPh_3)_7](NO_3)_2$ (**2**), the quantitative ligand exchange kinetics of **2** with tri-*p*-tolylphosphine, $P(p\text{-}C_6H_4CH_3)_3$, and analogous semiquantitative results for the new cluster $[(H)Pt(AuPPh_3)_9](NO_3)_2$ (**3**). The results of this study provide a more quantitative and improved understanding of the mechanism of catalytic H_2-D_2 equilibration.

Results and Discussion

To clarify the mechanism of H_2-D_2 equilibration catalyzed by **1**, a kinetic study of phosphine inhibition using another cluster compound was necessary. It was found that $[(H)(PPh_3)Pt(AuPPh_3)_7](NO_3)_2$ (**2**) would be a good subject for this study. Unlike **1**, this cluster is stable in the presence of excess PPh_3 and H_2. Cluster **2** is also a good H_2-D_2 equilibration catalyst (comparable in rate to **1**), and the mechanism of the reaction is assumed to be similar.[13] The fact that **2** is already an 18-electron hydride also makes the first step of hydrogen addition unnecessary, thereby simplifying the reaction kinetics. The mechanism shown in Scheme 1 is proposed for H_2-D_2 equilibration catalyzed by **2**. There is no distinction made or implied between the various bonding modes (terminal, bridging, or η^2) possible for hydrogen and deuterium in this mechanism.

Scheme 1. Proposed Mechanism for H_2-D_2 Equilibration Catalyzed by **2**

$$[(H)(PPh_3)Pt(AuPPh_3)_7](NO_3)_2 \underset{k_{-1}}{\overset{k_1}{\rightleftharpoons}} [(H)(PPh_3)Pt(AuPPh_3)_6Au](NO_3)_2 + PPh_3 \quad (1a)$$

$$[(H)(PPh_3)Pt(AuPPh_3)_6Au](NO_3)_2 + D_2 \xrightarrow{k_2} [(H)(D)_2(PPh_3)Pt(AuPPh_3)_6Au](NO_3)_2 \quad (1b)$$

$$[(H)(D)_2(PPh_3)Pt(AuPPh_3)_6Au](NO_3)_2 \xrightarrow{\text{fast}} [(D)(HD)(PPh_3)Pt(AuPPh_3)_6Au](NO_3)_2 \quad (1c)$$

$$[(D)(HD)(PPh_3)Pt(AuPPh_3)_6Au](NO_3)_2 \xrightarrow[\text{fast}]{k_{-2}} [(D)(PPh_3)Pt(AuPPh_3)_6Au](NO_3)_2 + HD \quad (1d)$$

Steps 1a and 1b of the mechanism involve dissociation of PPh_3 and binding of D_2, respectively. It is not possible from this kinetic analysis alone to determine if a PPh_3 ligand bonded to Au or Pt dissociates in step 1a. Indirect evidence suggests, however, that the phosphine dissociates from a Au atom (*vide infra*). Steps 1c and 1d of the catalytic process are assumed to be fast and have no influence on the rate of the reaction. We expect intramolecular scrambling of H and D in step 1c and elimination of HD in step 1d to be fast. The last assumption is based on the fact that the trihydride intermediates are not observable by spectroscopic techniques. This assumption will be further justified by consideration of the kinetic results below. Another assumption which we think is justified for this mechanism is the steady-state approximation for the species $[(H)(PPh_3)Pt(AuPPh_3)_6(Au)](NO_3)_2$. This is based on the unobservability of this species by spectroscopy indicating that its concentration is small and constant during the course of the reaction. This analysis provides a good background to study the kinetics of H_2-D_2 equilibration in the presence of added phosphine. It is, however, useful to first present the results of a ligand exchange rate study in order to provide justification for some of the above mechanistic assumptions.

Kinetics of Ligand Exchange with $[(H)(PPh_3)Pt(AuPPh_3)_7](NO_3)_2$ (2). Since a key step in the mechanism of H_2-D_2 equilibration involves phosphine dissociation (step 1a), the kinetics of phosphine ligand exchange for **2** was studied. This would permit an independent determination of the value of k_1 defined in step 1a of Scheme 1. A ligand exchange reaction (Scheme 2) was chosen because the first step of dissociative ligand exchange, step 2a, is the same as step 1a. The ligand exchange reaction shown in Scheme 2 is assumed to be dissociative because of steric crowding around the metal core and the known chemistry of Pt−Au clusters.[1] In Scheme 2, k_1 represents the rate constant for the dissociation of one PPh_3 ligand from an Au atom (vide infra) and PR_3 is $P(p\text{-}C_6H_4CH_3)_3$. It is assumed that the rates of dissociation of PPh_3 and PR_3 are equal (i.e., the values of k_1 in steps 2a and 2b are the same). We believe this assumption is valid because, in a solution of **2** with added PR_3 where the total moles of PR_3 and PPh_3 are equal, the equilibrium concentration of free PR_3 equals 50% of its initial value. In addition, the structural parameters (distances and angles in the metal core) of the related cluster $[Pt(AuPX_3)_8](NO_3)_2$ where X = Ph and $p\text{-}C_6H_4CH_3$ are the same within experimental error, showing that the $p\text{-}CH_3$ substitution does not cause significant structural changes.[15]

Scheme 2. Proposed Mechanism for Ligand Exchange with **2**

$$[(H)(PPh_3)Pt(AuPPh_3)_7](NO_3)_2 \underset{k_{-1}}{\overset{k_1}{\rightleftharpoons}} [(H)(PPh_3)Pt(AuPPh_3)_6(Au)](NO_3)_2 + PPh_3 \quad (2a)$$

$$[(H)(PPh_3)Pt(AuPPh_3)_6(Au)](NO_3)_2 + PR_3 \underset{k_1}{\overset{k_{-1}}{\rightleftharpoons}} [(H)(PPh_3)Pt(AuPPh_3)_6(AuPR_3)](NO_3)_2 \quad (2b)$$

Using this assumption and treating the species $[(H)(PPh_3)Pt(AuPPh_3)_6(Au)](NO_3)_2$ as a steady-state intermediate, one can derive the rate expressions for the reactions in Scheme 2. This type of ligand exchange process has been extensively studied by others.[16] The rate law for this general process with the above assumptions has been described in the literature,[16a−d] and given explicitly in ref 16a. It is shown in eq II. In this expression $[PPh_3]_\infty$ is the concentration of free PPh_3 at equilibrium, equaling 50% of C_{lig} in our experiment, C_{lig} is the total concentration of

(15) Krogstad, D. A.; Pignolet, L. H. Results to be published.

(16) (a) Helm, L.; Elding, L. I.; Merbach, A. E. *Inorg. Chem.* **1985**, *24*, 1719. (b) Espenson, J. H. *Chemical Kinetics and Reaction Mechanisms*; McGraw-Hill: New York, 1981; pp 50−55. (c) Frost, A. A.; Pearson, R. G. *Kinetics and Mechanism*, 2nd ed.; Wiley: New York, 1961; pp 192−193. (d) Wilkins, R. G. *Kinetics and Mechanisms of Reactions of Transition Metal Complexes*, 2nd ed.; VCH: New York, 1991; pp 38−61.

$$\ln\{1 - ([PPh_3]_t/[PPh_3]_\infty)\} = -k_1 t(C_{lig} + nC_{cluster})/nC_{lig} \quad \text{(II)}$$

free phosphine, $C_{cluster}$ is the total concentration of cluster, and n is the number of exchangeable phosphines and equals 7 for this case. Hence, plotting $\ln\{1 - ([PPh_3]_t/[PPh_3]_\infty)\}$ *vs* t should yield a straight line with slope $= -k_1(C_{lig} + 7C_{cluster})/7C_{lig}$. Figure 1 shows this plot from data determined by ^{31}P NMR integrations of signals due to free PPh_3 and $P(p\text{-}C_6H_4CH_3)_3$ as a function of time for **2**. This experiment was carried out with acetonitrile as solvent and is described in the Experimental Section. The slope determined from this plot is -8.37×10^{-5} s^{-1}, giving a value of $k_1 = 2.9 \times 10^{-4}$ s^{-1} after substitution of the known concentrations. Because ligand exchange kinetics for **2** were unaffected by the presence of a H_2 atmosphere, the above experiments were carried out in air.

Kinetics of PPh_3 Inhibition of H_2-D_2 Equilibration Catalyzed by 2. The rate law shown in Scheme 3 was derived from the mechanism in Scheme 1. In this rate law $[(H,D)_2]$ equals the total concentration of both hydrogen and deuterium and d[HD]/dt is the observed rate of HD production. An important assumption made in the rate law derivation is that recycling of the catalytically active species $[(H,D)(PPh_3)Pt(AuPPh_3)_6Au](NO_3)_2$ (step 1d) will not have an effect on the overall rate of the reaction. This assumption simplifies the kinetic analysis and is justified by the results presented below.[17]

Scheme 3. Rate Law Derived from the Mechanism Shown in Scheme 1

$$d[HD]/dt = k_{obs}[(H,D)_2] \quad \text{(3a)}$$

$$\text{giving} \qquad k_{obs} = \frac{k_1 k_2[\mathbf{2}]}{k_{-1}[PPh_3] + k_2[(H,D)_2]} \quad \text{(3b)}$$

$$\frac{1}{k_{obs}} = \frac{k_{-1}}{k_1 k_2[\mathbf{2}]}[PPh_3] + \frac{[(H,D)_2]}{k_1[\mathbf{2}]} \quad \text{(3c)}$$

To evaluate this rate law, different amounts of PPh_3 were added to the catalyst with use of nitrobenzene as solvent and rates of HD production measured (see Experimental Section). According to the rate expression derived in Scheme 3, the dependence of $1/k_{obs}$ on the concentration of added triphenylphosphine should be linear (eq 3c). The plot of these data is shown in Figure 2 and is in good agreement with the rate expression. The intercept of the $1/k_{obs}$ *vs* $[PPh_3]$ plot is 7.7×10^3 s and is equal to $[(H,D)_2]/k_1[\mathbf{2}]$ from eqn 3c. The value for k_1, the rate constant for phosphine dissociation from $[(H)(PPh_3)Pt(AuPPh_3)_7](NO_3)_2$, can be calculated from the value of the intercept, the known solubility of H_2 in nitrobenzene (9.7×10^{-4} M at 30 °C at $P = 760$ Torr),[13] and the concentration of **2** ($[\mathbf{2}] = 3.9 \times 10^{-4}$ M). The value determined for k_1 from this analysis is 3.1×10^{-4} s^{-1}.

The value of k_1 determined independently from the ligand exchange experiment (2.9×10^{-4} s^{-1}) is very close to the value determined from the H_2-D_2 equilibration rate study (3.1×10^{-4} s^{-1}). This agreement validates the assumptions made above[17] and provides strong support for the ligand dissociation step in the catalytic H_2-D_2 equilibration mechanism shown in Scheme 1. Some comment is needed on the fact that different solvents (nitrobenzene and acetonitrile) were used in these two kinetic studies. This was necessary for experimental reasons and should not cause significant differences in the rates.[18] In a previous kinetic study it was shown that the rates of H_2-D_2 equilibration are approximately the same for these two solvents, after correction for differences in H_2 solubility.[13]

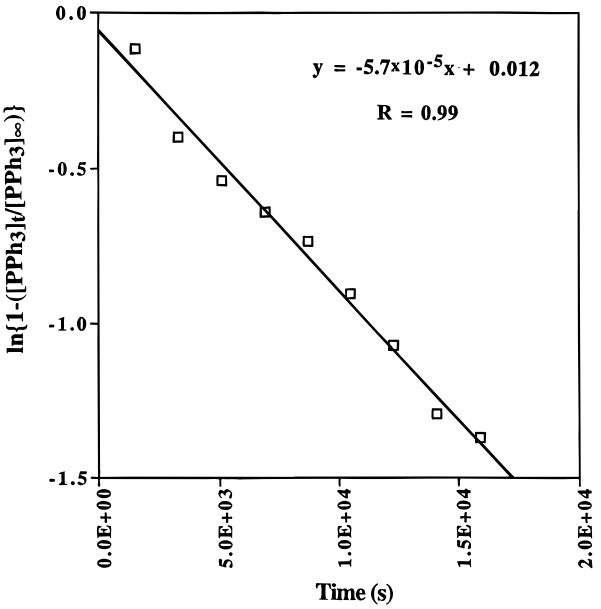

Figure 1. Plot of $\ln\{1 - ([PPh_3]_t/[PPh_3]_\infty)\}$ *vs* t for **2** according to the rate law for ligand exchange shown in eq II.

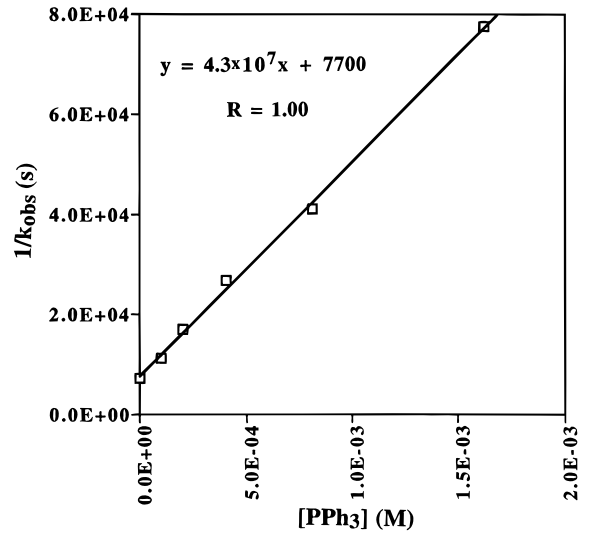

Figure 2. Plot of $1/k_{obs}$ for H_2-D_2 equilibration *vs* concentration of added PPh_3 for **2** as catalyst according to the rate law shown in Scheme 3.

Rate Studies of H_2-D_2 Equilibration and Ligand Exchange with $[(H)Pt(AuPPh_3)_9](NO_3)_2$ (3). The above rate measurements and analysis with **2** provided support for the

(17) If recycling of the catalyst is included (step 1d) in the rate law derivation, the denominator of expression 3b will include an additional term that contains the rate constant k_{-2} as follows: $k_{obs} = k_1k_2[\mathbf{2}]/\{k_{-1}[PPh_3] + k_2[(H,D)_2] - k_{-2}[M^*]\}$ where $M^* = [(D)(HD)(PPh_3)Pt(AuPPh_3)_6Au](NO_3)_2$. This will add a second term, $-\{k_{-2}[M^*]/k_1k_2[\mathbf{2}]\}$, to the intercept in the $1/k_{obs}$ *vs* $[PPh_3]$ plot of eq 3c. The intercept in eq 3c therefore becomes $\{[(H,D)_2]/k_1[\mathbf{2}]\} - \{k_{-2}[M^*]/k_1k_2[\mathbf{2}]\}$. It is shown in the analysis of all the rate data (ligand exchange and H_2-D_2 equilibration) that this additional component does not have a significant effect on the value of the intercept and therefore can be ignored. This is based on the observation that the k_1 values determined from ligand exchange and H_2-D_2 equilibration rate studies, with the exclusion of step 1d, were in close agreement.

(18) Nitrobenzene was used in the H_2-D_2 equilibration rate studies because of its low vapor pressure, which permitted accurate $(H,D)_2$ pressure determination and mass spectroscopic analysis of the reactor head space. Volatile solvents caused difficulty in these measurements. Acetonitrile was used in the ligand exchange studies because of increased cluster solubility and improved ^{31}P NMR resolution. It was not feasible to use nitrobenzene in the ligand exchange studies.

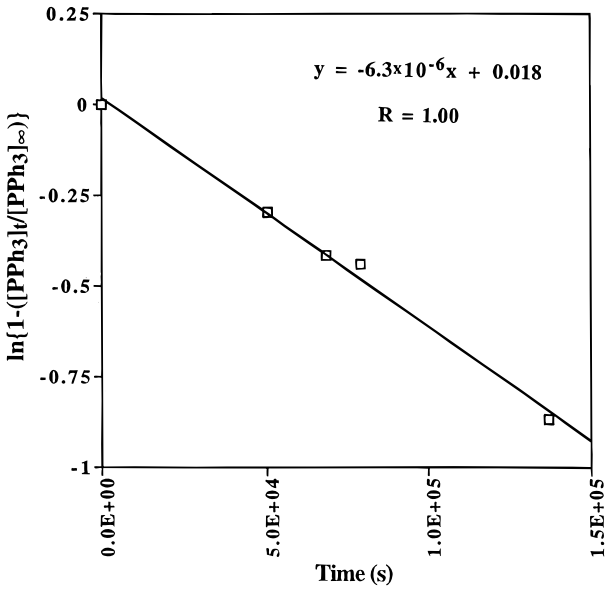

Figure 3. Plot of $\ln\{1 - ([PPh_3]_t/[PPh_3]_\infty)\}$ *vs t* for **3** according to the rate law for ligand exchange shown in eq II.

mechanism of H_2-D_2 equilibration shown in Scheme 1. A key feature of this mechanism involves phosphine dissociation to give a species with an open Au site (step 1a). Although the kinetic analysis assumed phosphine dissociation from Au, it is possible that PPh_3 dissociation from the Pt atom in **2** is kinetically important. The availability of a new hydrido cluster, $[(H)Pt(AuPPh_3)_9](NO_3)_2$ (**3**), that does not contain a PPh_3 ligand bonded to Pt permitted additional rate studies to address this question. The preparation and characterization of **3** are described in the next section.

The rate of H_2-D_2 equilibration was measured for **3** with nitrobenzene as solvent (30 °C, 760 Torr). The turnover frequency (TOF) was determined to be 5.5×10^{-3} s^{-1}. This rate is significantly slower than those determined for **1** and **2** under identical conditions (7.5×10^{-2} and 7.7×10^{-2} s^{-1}, respectively).[13] A quantitative phosphine inhibition study was not feasible for **3** because of its slow rate; however, a similar inhibition with added PPh_3 was observed qualitatively. A ligand exchange rate study with $P(p\text{-}C_6H_4CH_3)_3$ was carried out with **3** using the same experimental conditions and analysis as with **2**. The results of this experiment are shown by the plot of $\ln\{1 - ([PPh_3]_t/[PPh_3]_\infty)\}$ *vs t* in Figure 3. The value of k_1 (defined in Scheme 2 for **2**) determined from this plot (2.8×10^{-5} s^{-1}) is an order of magnitude smaller than the value determined for **2** above (3.3×10^{-4} s^{-1}), indicating that **3** exchanges triphenylphosphine ligands with $P(p\text{-}C_6H_4CH_3)_3$ at a much slower rate. The slower rate of ligand exchange for **3** compared to **2** provides evidence in favor of the proposed mechanism for H_2-D_2 equilibration shown in Scheme 1. According to eq 3b, the rate of HD production is directly proportional to the rate constant for phosphine dissociation, k_1. The ratio of k_1 values (k_1(**2**)/k_1(**3**) = 10) is similar to the ratio of rates for H_2-D_2 equilibration (TOF(**2**)/TOF(**3**) = 14).

The above result and the fact that **3** does not have a PPh_3 ligand bound to the Pt atom support the hypothesis that a key step in the mechanism for H_2-D_2 equilibration involves the dissociation of a PPh_3 ligand from a Au atom. In our original paper on this subject, evidence was presented that eliminated irreversible cluster fragmentation as a cause of the homogeneous H_2-D_2 equilibration catalysis.[13] It is more difficult to eliminate reversible cluster fragmentation. It is always possible that the dissociation of a small, undetectable fragment such as $AuPPh_3^+$ occurs and results in a more active catalyst. There are many results that argue against this however. First, we have examined a number of smaller clusters that would result from such a dissociation and in all cases the rate of H_2-D_2 equilibration is similar to or slower than that with the larger cluster. For example, $[(H)(PPh_3)Pt(AuPPh_3)_6](NO_3)$ has a turnover frequency of 2.1×10^{-2} s^{-1} compared with 7.7×10^{-2} s^{-1} for $[(H)(PPh_3)Pt(AuPPh_3)_7](NO_3)_2$.[13] In addition, it is known that PPh_3 reacts with $AuPPh_3^+$ to give the more stable $[Au(PPh_3)_2]^+$ cation. This species does not catalyze H_2-D_2 equilibration. Thus, if $AuPPh_3^+$ dissociated from **1**−**3**, the addition of PPh_3 would be expected to produce $[Au(PPh_3)_2]^+$ and increase cluster fragmentation. In the added PPh_3 inhibition experiments, no $[Au(PPh_3)_2]^+$ was observed by NMR and the rate of H_2-D_2 equilibration was slowed and not enhanced, in agreement with the rate law derived from the mechanism in Scheme 1.

Synthesis and Characterization of $[(H)Pt(AuPPh_3)_9](NO_3)_2$ (3). Cluster **3** was prepared by reaction of PPh_3 with $[(H)Pt(AuPPh_3)_8(AuPy)](NO_3)_2$ in methanol solution (Py = pyridine). This simple ligand substitution was unexpected because an earlier report claimed that Pt could not be surrounded by more than eight $AuPPh_3$ groups.[19] This was based on steric arguments. The precursor cluster $[(H)Pt(AuPPh_3)_8(AuPy)](NO_3)_2$ was previously prepared by Kappen et al.[6] and is an excellent starting point for the synthesis of new clusters.

Compound **3** was characterized by elemental analysis, fast-atom bombardment mass spectroscopy (FABMS), ^{31}P and ^1H NMR spectroscopy, and single-crystal X-ray crystallography. A summary of the crystal data for **3** is presented in Table 1. A thermal ellipsoid representation of the cluster core, selected positional and thermal parameters, and selected distances and angles are shown in Figures 4 and 5 and Tables 2 and 3. Although the location of the hydride ligand could not be determined from the X-ray structure analysis, its presence is clearly evident in the ^1H NMR spectrum (Figure 6) and from the diamagnetic nature of the cluster (*vide infra*).

Compound **3** is a doubly charged, 18-electron monohydrido $PtAu_9$ cluster. As with most other platinum−gold clusters of this type, the molecule is platinum-centered with the nine $AuPPh_3$ groups positioned around Pt in a distorted icosahedral arrangement. It follows the predicted trend in metal-centered gold cluster chemistry that 18-electron clusters have a spheroidal geometry.[1−9] An interesting feature of the crystal structure is that the cluster crystallized as two different isomers in the asymmetric unit. These isomers (labeled with primed and unprimed atom symbols) have significant structural differences in terms of the placement of gold atoms around the platinum center. In both molecules, six $AuPPh_3$ groups are arranged so that they approximately form one capped pentagonal face of an icosahedron. This is illustrated most clearly in the bottom views of Figures 4 and 5, where Au(7) is capping the pentagonal face. The positioning of the other three $AuPPh_3$ units (Au(2), Au(3), and Au(5)) shows significant variation. This is best seen in the "top" views of the thermal ellipsoid structures in Figures 4 and 5. Note that the Au(2)−Au(3) distance is 3.107 Å while the Au(2′)−Au(3′) distance is 3.988 Å. The average Pt−Au distances are similar for both isomers (2.687(1) and 2.684(1) Å for primed and unprimed molecules, respectively) and are comparable to average Pt−Au distances in the other 18-electron Pt−Au clusters (for example, 2.675 Å in $[(CO)Pt(AuPPh_3)_8](NO_3)_2$,[20] 2.687 Å in $[(CO)(PPh_3)Pt(AuPPh_3)_6](NO_3)_2$,[21] and

(19) Steggerda, J. J.; Bour, J. J.; van der Velden, J. W. A. *Recl. Trav. Chim. Pays-Bas* **1982**, *101*, 164.
(20) Kanters, R. P. F.; Schlebos, P. P. J.; Bour, J. J.; Bosman, W. P.; Behm, H. J.; Steggerda, J. J. *Inorg. Chem.* **1988**, *27*, 4034.
(21) Ito, L. N.; Sweet, J. D.; Mueting, A. M.; Pignolet, L. H.; Schoondergang, M. F. J.; Steggerda, J. J. *Inorg. Chem.* **1989**, *28*, 3696.

Table 1. Crystallographic Data for $[(H)Pt(AuPPh_3)_9](NO_3)_2 \cdot 0.5(C_2H_5)_2O$ (**3**)

Crystal Parameters and Measurement of Intensity Data	
empirical formula	$C_{164}H_{141}Au_9N_2O_{6.5}P_9Pt$
fw	4489.30
temp	173(2) K
wavelength (Mo Kα)	0.71073
space group	$P\bar{1}$ (No. 2)
cell params	$a = 17.0452(1)$ Å, $b = 17.4045(2)$ Å, $c = 55.2353(1)$ Å $\alpha = 89.891(1)°$, $\beta = 85.287(1)°$, $\gamma = 75.173(1)°$
cell vol	15784.0(2) Å^3
Z	4
calcd density	1.889 Mg m^{-3}
abs coeff	9.357 mm^{-1}
max, min trans factors	0.234, 0.096
Refinement[a] by Full-Matrix Least-Squares Calculations on F^2	
data/params	45929/3367
final R indices [$I > 2\sigma(I)$]	R1 = 0.0892, wR2 = 0.1794[b]

[a] Relevant equations: $R1 = \sum||F_o| - |F_c||/\sum|F_o|$, $wR2 = \{\sum[w(F_o^2 - F_c^2)^2]/\sum[w(F_o^2)^2]\}^{1/2}$, where $w = q/\sigma^2(F_o^2) + (ap)^2 + bp$. [b] Refinements are performed wtih F^2 (rather than F), enabling all data to be used, with the result that the experimental information is more fully exploited. Note that the wR2 index which is minimized during the refinement is for statistical reasons about twice as large as the conventional R index R1.

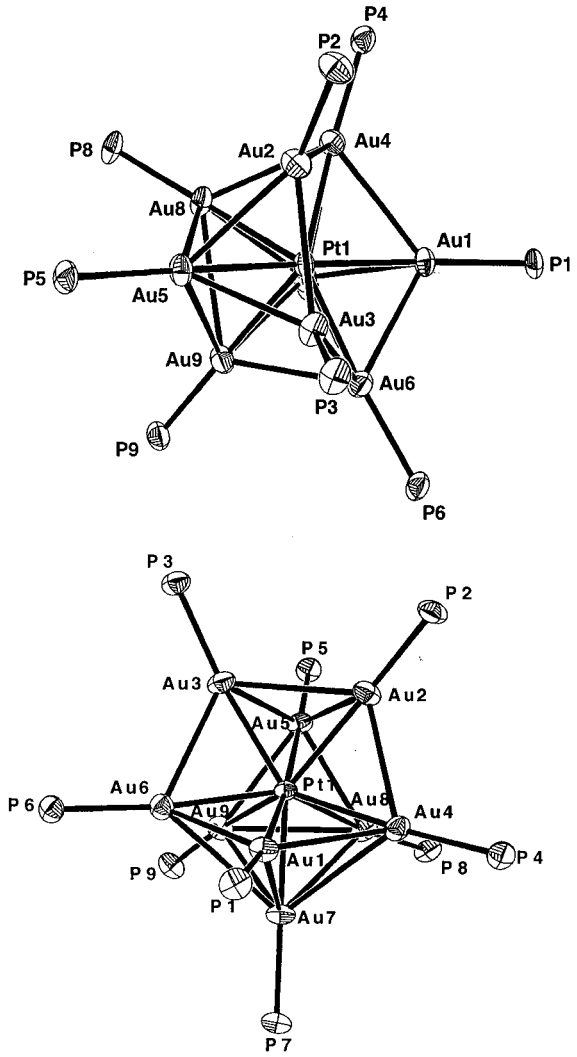

Figure 4. Thermal ellipsoid drawings of the unprimed isomer of **3**. In the top view, the Au(7)−P(7) bond points into the paper behind the Pt atom. Thermal ellipsoids are drawn with 50% probability boundaries.

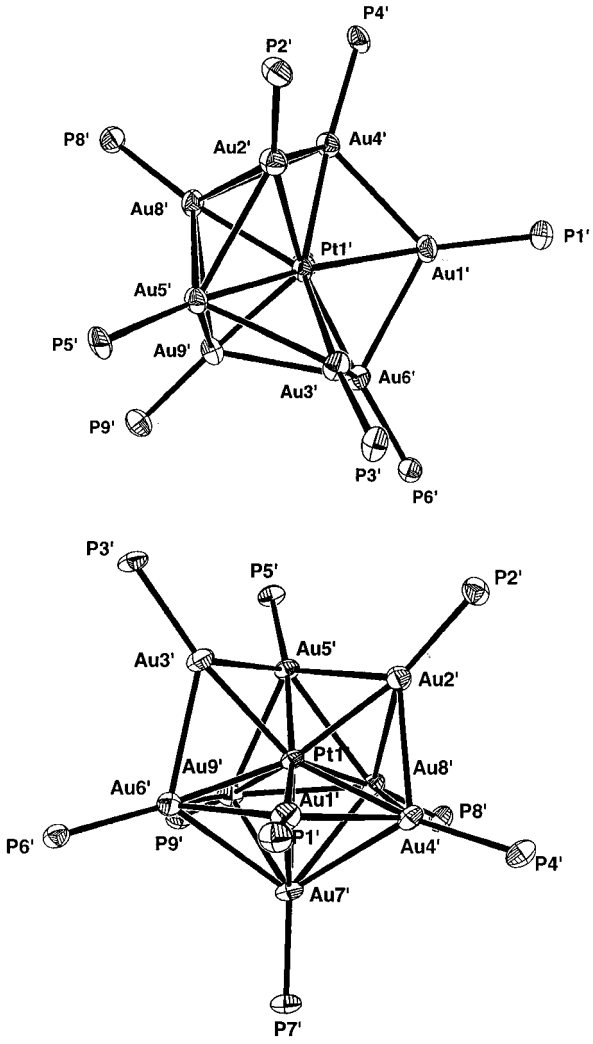

Figure 5. Thermal ellipsoid drawings of the primed isomer of **3**. In the top view, the Au(7′)−P(7′) bond points into the paper behind the Pt atom. Thermal ellipsoids are drawn with 50% probability boundaries.

2.702 Å in **2**[22]). The average Pt−Au distances in 16-electron clusters are somewhat shorter (for example, 2.635 Å in **1**).[23] The Au−Au distances show large variation within and between the two isomers (most notably involving Au(2), Au(3), and Au(5)) but are comparable to values in other Pt−Au clusters.[1−9] The interactions between adjacent Au atoms in M−Au and Au clusters are rather soft, accounting for this large variation in Au−Au distance.[1−9] The average Au−P distances (2.308(6) and 2.315(6) Å for the two isomers) are in the range generally

(22) Kanters, R. P. F.; Bour, J. J.; Schlebos, P. P. J.; Bosman, W. P.; Behm, H.; Steggerda, J. J.; Ito, L. N.; Pignolet, L. H. *Inorg. Chem.* **1989**, *28*, 2591.
(23) Bour, J. J.; Kanters, R. P. F.; Schlebos, P. P. J.; Steggerda, J. J. *Recl. Trav. Chim. Pays-Bas* **1988**, *107*, 211.

Table 2. Selected Atomic Coordinates ($\times 10^4$) and Equivalent Isotropic Displacement Parameters ($Å^2 \times 10^3$) for **3**

atom	*x*	*y*	*z*	U_{eq}[a]
Pt(1)	3996(1)	2807(1)	1338(1)	20(1)
Au(1)	3536(1)	3565(1)	1773(1)	27(1)
Au(2)	2666(1)	2660(1)	1135(1)	31(1)
Au(3)	3873(1)	1316(1)	1388(1)	31(1)
Au(4)	2941(1)	4213(1)	1288(1)	29(1)
Au(5)	4350(1)	1893(1)	924(1)	27(1)
Au(6)	4824(1)	2062(1)	1695(1)	29(1)
Au(7)	4832(1)	3869(1)	1430(1)	28(1)
Au(8)	4316(1)	3542(1)	930(1)	29(1)
Au(9)	5608(1)	2241(1)	1219(1)	30(1)
P(1)	3011(4)	3999(4)	2160(1)	30(2)
P(2)	1321(4)	2689(4)	1102(1)	33(2)
P(3)	3538(4)	137(4)	1442(1)	33(2)
P(4)	1928(4)	5383(4)	1261(1)	31(2)
P(5)	4644(4)	1082(4)	574(1)	32(2)
P(6)	5381(4)	1352(4)	2018(1)	30(1)
P(7)	5539(4)	4797(4)	1518(1)	29(1)
P(8)	4523(5)	4084(4)	557(1)	33(2)
P(9)	7003(4)	1870(4)	1129(1)	33(2)
Pt(1′)	2533(1)	2756(1)	6256(1)	19(1)
Au(1′)	1450(1)	3095(1)	6647(1)	27(1)
Au(2′)	1679(1)	3278(1)	5876(1)	27(1)
Au(3′)	2448(1)	1220(1)	6209(1)	27(1)
Au(4′)	1638(1)	4239(1)	6295(1)	25(1)
Au(5′)	3230(1)	2034(1)	5839(1)	23(1)
Au(6′)	3025(1)	1852(1)	6628(1)	25(1)
Au(7′)	3122(1)	3592(1)	6570(1)	27(1)
Au(8′)	3203(1)	3742(1)	5986(1)	26(1)
Au(9′)	4176(1)	2294(1)	6240(1)	26(1)
P(1′)	346(4)	3157(4)	6924(1)	29(1)
P(2′)	720(4)	3475(4)	5598(1)	30(1)
P(3′)	2178(4)	3(3)	6138(1)	26(1)
P(4′)	683(4)	5523(4)	6307(1)	28(1)
P(5′)	3841(4)	1275(4)	5501(1)	25(1)
P(6′)	3353(4)	1009(4)	6947(1)	26(1)
P(7′)	3621(4)	4309(4)	6849(1)	27(1)
P(8′)	3678(4)	4747(4)	5797(1)	29(1)
P(9′)	5587(4)	1832(4)	6222(1)	30(1)

[a] U_{eq} is defined as one-third of the trace of the orthogonalized $\mathbf{U}_{ij}$ tensor.

found for PPh_3-ligated Pt−Au cluster compounds.[1−9] In summary, the structure of **3** is not unusual, with geometric parameters well within their expected ranges. This indicates that the placement of nine $AuPPh_3$ groups around Pt does not lead to a significant structural distortion as might be expected from increased steric crowding. The observation of two different structural isomers is interesting but consistent with the soft Au−Au bonding and well-known solution fluxionality found in M−Au clusters of this type.[1−9]

The results of the X-ray structure determination did not suggest where the hydrogen ligand is positioned. Hydrogen ligands in Pt−Au clusters are believed to bridge Pt−Au bonds, and this is likely to be the case in **3**.[1,22] There is no IR evidence for a terminal Pt−H, and the ^{1}H NMR data are similar to those for other Pt−Au hydrido clusters. The ^{1}H NMR resonance assigned to the hydrogen ligand in **3** is shown in Figure 6. It consists of an even multiplet (eight of the expected ten lines observed) with ^{195}Pt satellites (δ = 2.25 ppm, $^3J_{H-P}$ = 13.5 Hz, $^1J_{H-Pt}$ = 627 Hz). These values (δ, $^3J_{H-P}$, $^1J_{H-Pt}$) are comparable to those observed for **2** (2.26 ppm, 16.6 Hz, 537 Hz),[20] $[(H)Pt(AuPPh_3)_8](NO_3)$ (5.4 ppm, 14.3 Hz, 705 Hz),[24] and $[(H)(PPh_3)Pt(AuPPh_3)_6](NO_3)$ (0.34 ppm, 18.3 Hz, 687 Hz).[24] The unusual downfield shift for these hydrogen ligands has not been explained but is typical for M−Au cluster compounds.[1,6,7,11,24,25]

In most phosphine-ligated M−Au clusters, the PPh_3 ligands are equivalent on the NMR time scale because of rapid skeletal rearrangement of the $AuPPh_3$ groups.[1−9] The ^{31}P{^{1}H} NMR spectrum of **3** at ambient temperature therefore consists of a singlet (δ = 50.4 ppm) with the usual ^{195}Pt satellites ($^2J_{P-Pt}$ = 403 Hz). These values are typical of other 18-electron hydrido Pt−Au clusters (for example, **2** (δ = 45.7 ppm, $^2J_{P-Pt}$ = 414 Hz),[22] $[(H)Pt(AuPPh_3)_8](NO_3)$ (52.1 ppm, 452 Hz),[24] and $[(H)(PPh_3)Pt(AuPPh_3)_6](NO_3)$ (48.2 ppm, 457 Hz)).[24] At −90 °C

Table 3. Selected Bond Distances and angles with Estimated Standard Deviations for **3**

Bond Distances (Å)

Pt(1)−Au(1)	2.702(1)	Pt(1′)−Au(1′)	2.684(1)
Pt(1)−Au(2)	2.679(1)	Pt(1′)−Au(2′)	2.680(1)
Pt(1)−Au(3)	2.668(1)	Pt(1′)−Au(3′)	2.728(1)
Pt(1)−Au(4)	2.669(1)	Pt(1′)−Au(4′)	2.719(1)
Pt(1)−Au(5)	2.726(1)	Pt(1′)−Au(5′)	2.664(1)
Pt(1)−Au(6)	2.660(1)	Pt(1′)−Au(6′)	2.645(1)
Pt(1)−Au(7)	2.680(1)	Pt(1′)−Au(7′)	2.679(1)
Pt(1)−Au(8)	2.672(1)	Pt(1′)−Au(8′)	2.681(1)
Pt(1)−Au(9)	2.697(1)	Pt(1′)−Au(9′)	2.702(1)
Au(1)−Au(4)	3.054(1)	Au(1′)−Au(4′)	2.906(1)
Au(1)−Au(6)	2.959(1)	Au(1′)−Au(6′)	2.981(1)
Au(1)−Au(7)	2.939(1)	Au(1′)−Au(7′)	3.180(1)
Au(2)−Au(3)	3.107(1)	Au(2′)−Au(3′)	3.988(1)
Au(2)−Au(4)	2.994(1)	Au(2′)−Au(4′)	2.902(1)
Au(2)−Au(5)	2.980(1)	Au(2′)−Au(5′)	2.949(1)
Au(2)−Au(8)	3.640(1)	Au(2′)−Au(8′)	3.018(1)
Au(3)−Au(5)	2.883(1)	Au(3′)−Au(5′)	2.911(1)
Au(3)−Au(6)	2.953(1)	Au(3′)−Au(6′)	2.912(1)
Au(3)−Au(9)	3.766(1)	Au(3′)−Au(9′)	3.886(1)
Au(4)−Au(7)	3.285(1)	Au(4′)−Au(7′)	3.041(1)
Au(4)−Au(8)	2.933(1)	Au(4′)−Au(8′)	2.984(1)
Au(5)−Au(8)	2.856(1)	Au(5′)−Au(8′)	3.069(1)
Au(5)−Au(9)	2.978(1)	Au(5′)−Au(9′)	2.944(1)
Au(6)−Au(7)	3.469(1)	Au(6′)−Au(7′)	3.089(1)
Au(6)−Au(9)	2.905(1)	Au(6′)−Au(9′)	3.020(1)
Au(7)−Au(8)	3.064(1)	Au(7′)−Au(8′)	3.233(1)
Au(7)−Au(9)	2.998(1)	Au(7′)−Au(9′)	3.011(1)
Au(8)−Au(9)	3.243(1)	Au(8′)−Au(9′)	3.048(1)
Au(1)−P(1)	2.300(6)	Au(1′)−P(1′)	2.308(6)
Au(2)−P(2)	2.302(6)	Au(2′)−P(2′)	2.294(6)
Au(3)−P(3)	2.280(6)	Au(3′)−P(3′)	2.320(6)
Au(4)−P(4)	2.322(6)	Au(4′)−P(4′)	2.331(6)
Au(5)−P(5)	2.337(6)	Au(5′)−P(5′)	2.304(6)
Au(6)−P(6)	2.297(6)	Au(6′)−P(6′)	2.303(6)
Au(7)−P(7)	2.322(6)	Au(7′)−P(7′)	2.327(6)
Au(8)−P(8)	2.304(6)	Au(8′)−P(8′)	2.320(6)
Au(9)−P(9)	2.310(7)	Au(9′)−P(9′)	2.327(7)

Bond Angles (deg)

Pt(1)−Au(1)−P(1)	167.9(2)	Pt(1′)−Au(1′)−P(1′)	163.8(2)
Pt(1)−Au(2)−P(2)	159.0(2)	Pt(1′)−Au(2′)−P(2′)	162.7(2)
Pt(1)−Au(3)−P(3)	170.3(2)	Pt(1′)−Au(3′)−P(3′)	170.5(2)
Pt(1)−Au(4)−P(4)	174.5(2)	Pt(1′)−Au(4′)−P(4′)	169.8(2)
Pt(1)−Au(5)−P(5)	178.6(2)	Pt(1′)−Au(5′)−P(5′)	173.4(2)
Pt(1)−Au(6)−P(6)	171.9(2)	Pt(1′)−Au(6′)−P(6′)	174.5(2)
Pt(1)−Au(7)−P(7)	178.8(2)	Pt(1′)−Au(7′)−P(7′)	178.9(2)
Pt(1)−Au(8)−P(8)	173.6(2)	Pt(1′)−Au(8′)−P(8′)	171.0(2)
Pt(1)−Au(9)−P(9)	174.6(2)	Pt(1′)−Au(9′)−P(9′)	177.2(2)

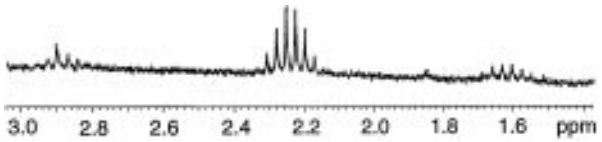

Figure 6. ^{1}H NMR spectrum of the hydride ligand **3** recorded at 500 MHz.

(24) Bour, J. J.; Schlebos, P. P. J.; Kappen, T. G. M. M.; Bosman, W. P.; Smits, J. M. M.; Beurskens, P. T.; Steggerda, J. J. *Inorg. Chim. Acta* **1990**, *171*, 177.

(25) Alexander, B. D.; Johnson, B. J.; Johnson, S. M.; Casalnuovo, A. L.; Pignolet, L. H. *J. Am. Chem. Soc.* **1986**, *108*, 4409.

some line-broadening is observed in the $^{31}P\{^1H\}$ NMR spectrum of **3**, but distinct phosphorus environments cannot be resolved. The isomers found in the crystal structure of **3** are just two of the many possibilities during fast skeletal rearrangement occurring in solution. It is not surprising that two are trapped in a single crystal. The FABMS of **3** and its mono(*p*-tolylphosphine) analog, $[(H)Pt(AuPPh_3)_8AuP(p\text{-}C_6H_4CH_3)_3](NO_3)_2$, gave fragmentation patterns consistent with their formulations.

Conclusions

The synthesis of the first Pt-centered cluster with nine $AuPPh_3$ groups directly bonded to the Pt has been achieved. Previously, clusters with up to eight $AuPPh_3$ groups were known. This new cluster **3** is a catalyst for H_2-D_2 equilibration in homogeneous solution phase and has proved helpful in our studies on the mechanism of this catalysis reaction. Phosphine inhibition and ligand exchange kinetic experiments have provided strong evidence in favor of the mechanism shown in Scheme 1. A key step in this mechanism is the dissociation of a PPh_3 ligand from Au to give an open site for bonding of H_2 or D_2. In this paper we have shown that the rate constant for phosphine dissociation (k_1 in eq 1a) determined from a PPh_3 inhibition rate study of H_2-D_2 equilibration with cluster **2** was nearly identical to the rate constant for phosphine ligand exchange for **2** (k_1 in Scheme 2). In addition, the rate law derived from the mechanism in Scheme 1 fits all of the observed kinetic data. The slower rate for H_2-D_2 equilibration observed with **3** is explained by its slower rate of phosphine ligand dissociation. Cluster **2** contains a PPh_3 ligand bonded to Pt, so there is a possibility that this was the PPh_3 ligand dissociating in step a of the mechanism. Since cluster **3** contains only Au-bonded PPh_3 ligands, the above result also supported $Au-PPh_3$ dissociation in Scheme 1 for cluster **2**.

The fact that clusters **2** and **3** show similar kinetic behaviors for H_2-D_2 equilibration suggests that the mechanism in Scheme 1 is general for 18-electron hydrido $Pt-AuPPh_3$ clusters. The related 16-electron cluster **1** reacts reversibly with H_2 to give the 18-electron dihydrido cluster $[(H)_2Pt(AuPPh_3)_8](NO_3)_2$. It is interesting that NMR ligand exchange studies with **1** showed no exchange with added $P(p\text{-}C_6H_4CH_3)_3$ under a N_2 or air atmosphere but measurable exchange upon the addition of H_2. Although a quantitative kinetic analysis was not possible with **1** because of cluster instability in the presence of added phosphine and H_2, we believe the mechanism shown in eq I is consistent with all of the available data. The reversible addition of H_2 to **1** has been shown to be fast and non-rate-limiting for H_2-D_2 equilibration.[13]

The results of this study are important. H_2-D_2 equilibration is being used as a probe reaction for H_2 activation with heterometallic clusters in solution and on solid supports.[1,13,14] It is therefore important to understand the details of the mechanism. For example, 16-electron clusters such as **1** immobilized intact on a silica support show significant activity (TOF = 220 s^{-1} at 25 °C, 1 atm) for heterogeneous H_2-D_2 equilibration catalysis only after pretreatment under a H_2 flow.[14] The 18-electron cluster **2** immobilized on silica is active (TOF = 170 s^{-1} at 25 °C, 1 atm) without the H_2 pretreatment.[14] The results of the mechanistic study in this paper have led to the proposal that the support assists in ligand dissociation from 18-electron hydrogen-containing clusters. This hypothesis is under current investigation.

Experimental Section

Physical Measurements and Reagents. ^{31}P NMR spectra were recorded with a Varian VX-300 spectrometer at 121.4 MHz. ^{31}P NMR spectra were run with proton decoupling, and shifts are reported in ppm relative to the internal standard trimethyl phosphate (TMP), with positive shifts downfield. ^1H NMR spectra were recorded on a Varian VX-500 spectrometer at 500 MHz with tetramethylsilane (TMS) as the internal standard. FABMS measurements were carried out with a VG Analytical 7070E-HF high-resolution, double-focusing mass spectrometer equipped with a VG 11/250 data system. FABMS samples were introduced in a *m*-nitrobenzyl alcohol matrix. Solvents were dried and distilled prior to use. The cluster compounds $[Pt(AuPPh_3)_8]_2(NO_3)_2$ (**1**), $[(H)(PPh_3)Pt(AuPPh_3)_7](NO_3)_2$ (**2**), and $[(H)Pt(AuPPh_3)_8(AuPy)](NO_3)_2$ were prepared as described in the literature.[6,19,22] Prepurified H_2 obtained from Linde (purity >99.99%) and CP grade D_2 obtained from Matheson (purity >99.5%) were passed through liquid-nitrogen traps to remove H_2O and O_2 impurities. Gas handling and mixing were carried out with electronic mass flow controllers and an RXM-100 high-vacuum gas-handling system (Advanced Scientific Designs). Gas transfers were carried out with the use of copper tubing plumbed directly into the reaction vessel and gas-handling system. Analysis of gas mixtures was accomplished by using mass spectrometer with a modified inlet system (Leybold Inficon Quadrex 200 residual gas analyzer) precalibrated for analyzing $H_2/HD/D_2$ mixtures. All other chemicals were of reagent grade and were used without further purification.

Preparations and Characterizations of Compounds. $[(H)Pt(AuPPh_3)_8](NO_3)_2$ (3). $[(H)Pt(AuPPh_3)_8(AuPy)](NO_3)_2$ (50 mg, 12 μmol) was dissolved in 15 mL of methanol. PPh_3 (3.2 mg, 12 μmol) was added to this solution and the mixture stirred for 1 h. Slow addition of diethyl ether precipitated the orange product in 85% yield. ^{31}P NMR (CD_3OD): singlet $\delta = 50.4$ ppm with Pt satellites $^2J_{P-Pt} = 403$ Hz. ^1H NMR (CD_3OD) of hydrido ligand: even multiplet $\delta = 2.25$ ppm, $^3J_{H-P} = 13.5$ Hz, $^1J_{H-Pt} = 627$ Hz. FABMS, *m/z*: 4453.4 calcd for $[(H)Pt(AuPPh_3)_9(NO_3)_2 = M]^+$, unobserved; 4328.4 calcd for $\{M - [H(NO_3)_2]\}^+$, 4328.6 obsd; 4066.3 calcd for $\{M - [H(NO_3)_2PPh_3]\}^+$, 4066.4 obsd; 3804.2 calcd for $\{M - [H(NO_3)_2(PPh_3)_2]\}^+$, 3804.1 obsd; 3542.1 calcd for $\{M - [H(NO_3)_2(PPh_3)_3]\}^+$, 3541.6 obsd. Anal. Calcd for $C_{162}H_{136}Au_9N_2O_6P_9Pt$: C, 43.69; H, 3.08; N, 0.63. Found: C, 42.58; H, 2.96; N, 0.69. Low carbon analysis is frequently found for compounds of this type.

$[(H)Pt(AuPPh_3)_8AuP(p\text{-}C_6H_4CH_3)_3](NO_3)_2$. This analog of **3** was prepared by the same procedure as for **3** but with $P(p\text{-}C_6H_4CH_3)_3$ substituted for PPh_3 in the second step. It was prepared to verify the FABMS assignment of **3**. ^{31}P NMR (CD_3OD): doublet $\delta = 50.3$ ppm with Pt satellites $^4J_{P-P} = 11$ Hz, $^2J_{P-Pt} = 403$ Hz assigned to the PPh_3 ligands (resonances due to the $P(p\text{-}C_6H_4CH_3)_3$ ligand were obscured by the much larger PPh_3 signals). FABMS, *m/z*: 4495.4 calcd for $[(H)Pt(AuPPh_3)_8(AuP(p\text{-}C_6H_4CH_3)_3)](NO_3)_2 = M]^+$, unobserved; 4370.9 calcd for $\{M - [H(NO_3)_2]\}^+$, 4369.8 obsd; 4108.8 calcd for $\{M - [H(NO_3)_2PPh_3]\}^+$, 4107.7 obsd; 3846.6 calcd for $\{M - [H(NO_3)_2(PPh_3)_2]\}^+$, 3845.6 obsd; 3584.5 calcd for $\{M - [H(NO_3)_2(PPh_3)_3]\}^+$, 3583.2 obsd; 4066.3 calcd for $\{M - [H(NO_3)_2P(p\text{-}C_6H_4CH_3)_3]\}^+$, 4065.7 obsd; 3804.2 calcd for $\{M - [H(NO_3)_2PPh_3P(p\text{-}C_6H_4CH_3)_3]\}^+$, 3803.5 obsd; 3542.1 calcd for $\{M - [H(NO_3)_2(PPh_3)_2P(p\text{-}C_6H_4CH_3)_3]\}^+$, 3541.0 obsd.

H_2-D_2 Equilibration Kinetic Measurements. The details of the experimental conditions, controls, and calculations for the measurement of the turnover frequency were reported previously.[13] The identical procedures and data workup were used in this study, so only some of the procedures and details are described here. For all of the rate measurements, the reactor was a 30-mL jacketed glass vessel equipped with a star-shaped Teflon stir bar, a gas-inlet tube connected to a vacuum/gas-handling system, and a rubber septum for gas sampling. The temperature of the reactor was held at 30 ± 0.2 °C. Dried and freshly distilled nitrobenzene was used as the solvent for all H_2-D_2 equilibration rate measurements. Sample preparation for the PPh_3 inhibition rate studies with **2** and **3** was performed as follows. A stock solution of PPh_3 dissolved in nitrobenzene (typically 10.0 mg in a 5.0 or 10.0 mL volumetric flask) was freshly prepared. A known amount of cluster, typically 16 mg, was dissolved in a small amount of nitrobenzene in a 10.0 mL volumetric flask. The appropriate volume of the stock PPh_3 solution was added by syringe, followed by dilution to the mark with nitrobenzene. A 6.0 mL volume of this solution was placed in the reactor and degassed by pumping for 5 min. Time zero for the kinetic run was defined as the time the reactor was charged with an equimolar mixture of H_2 and D_2 at 760 Torr total pressure.

The relative amounts of H_2, D_2, and HD in the head space of the reaction vessel were determined periodically by mass spectroscopy. Rate constants for HD production (k_{obs}) were determined by plotting the equation $\ln\{[HD]_e/([HD]_e - [HD]_t)\} = k_{obs}t$, where $[HD]_e$ and $[HD]_t$ are the mole fractions of HD at equilibrium and at time t, respectively. A typical plot for one of the PPh_3 inhibition experiments is shown as Figure S1 of the Supporting Information. The rate of HD production in (mol of HD)/s is defined as k_{obs}\{mol of $(H_2 + D_2 + HD)$\} where the mol of $(H_2 + D_2 + HD)$ in the reactor is 1.31×10^{-3}. The turnover rate is defined as the rate of HD production divided by the moles of cluster in the reactor and has the units of (mol of HD produced) (mol of cluster)$^{-1}$ s^{-1}.[13] The rate data for the PPh_3 inhibition study with cluster **2** are shown in Figure 1 as a $1/k_{obs}$ *vs* $[PPh_3]$ plot. The turnover rates for **2** are precise to ±5% as determined from repetitive runs.[13] The actual data used in this analysis are shown in Table S6 of the Supporting Information. In the case of **3**, the error is larger (estimated to be ±15%) because of the presence of a small amount of **1** as an impurity. The error in the rate constant k_1 (defined in eq 1a) is estimated to be ±15% by propagating the various errors in the analysis.

Ligand Exchange Kinetic Measurements. The ligand exchange reaction of **1** with $P(p\text{-}C_6H_4CH_3)_3$ was studied in CD_3CN solution at ambient temperature under an atmosphere of air and under an atmosphere of H_2. For both experiments, 10 mg (2.5 μmol) of **1** was placed in an NMR tube to which was added 1.0 mL of a CD_3CN solution that contained 1.5 mg (5.7 μmol) of $P(p\text{-}C_6H_4CH_3)_3$. The solution for the experiment run under H_2 was freeze-pump-thawed several times and charged with 1 atm of H_2, and the tube was sealed with use of a J. Young valve. ^{31}P NMR spectra were taken every hour for the first 4 h and then after 1 day. For the sample under air, no changes were observed, indicating that ligand exchange did not occur. For the sample under H_2, decomposition into $AuPPh_3^+$, $Au(PPh_3)_2^+$, and unidentified compounds occurred after several hours. Ligand exchange studies with **2** were carried out with a similar procedure but with 2.5 μmol of **2** and 17.5 μmol of $P(p\text{-}C_6H_4CH_3)_3$ and only under an air atmosphere. ^{31}P NMR spectra were taken every 30 min with NMR delays (d_1 = 2.5 s) selected to minimize integration error. Integrals of peaks corresponding to free $P(p\text{-}C_6H_4CH_3)_3$ ($\delta = -10$ ppm) and PPh_3 ($\delta = -8$ ppm) were monitored. Ligand exchange studies with **3** were conducted similarly but with 1.12 μmol of **3** and 10.1 μmol of $P(p\text{-}C_6H_4CH_3)_3$ in 1 mL of CD_3CN. The rate data determined from these experiments are shown in the $\ln\{[1 - ([PPh_3]/[PPh_3]_\infty)\}$ *vs* *t* plots in Figures 1 and 3 and in Table S7 of the Supporting Information. The estimated errors in the values of k_1 (defined in Scheme 2) are ±15%. These estimates were made by propagating errors in the analysis.

X-ray Structural Determination of $[(H)Pt(AuPPh_3)_9](NO_3)_2 \cdot 0.5(C_2H_5)_2O$. Data collection and structure solution were conducted at the X-Ray Crystallographic Laboratory of the University of Minnesota under the direction of Dr. Victor J. Young, Jr. All calculations were performed by using SGI INDY R4400-SC and CRAY-2 computers and the SHELXTL V5.0 suite of programs.[26]

Data Collection. A crystal of the compound attached to a glass fiber was mounted on a Siemens SMART CCD area detector system for data collection at 173(2) K. An initial set of cell constants were calculated from reflections harvested from three sets of 20−30 frames. These initial sets of frames were oriented such that orthogonal wedges of reciprocal space were surveyed. This produced orientation matrices determined from 50−300 reflections. Final cell constants were calculated from a set not exceeding 8192 strong reflections. Final cell constants reported in this manner are about 1 order of magnitude better in precision than those reported from four-circle diffractometers. The data collection technique used for this specimen is generally known as a hemisphere collection. Here a randomly oriented region of reciprocal space is surveyed to the extent of 1.3 hemispheres to a resolution of 0.87 Å. Three major swaths of frames are collected with 0.30° steps in ω. This collection strategy provides a high degree of redundancy. The redundant data provide good *y* input for an empirical absorption correction (see Table 1).

Structure Solution and Refinement. The space group $P\bar{1}$ (No. 2) was determined on the basis of systematic absences and intensity statistics. A successful direct-methods solution was calculated, which provided most non-hydrogen atoms from the *E* map. Several full-matrix least-squares/difference Fourier cycles were performed, which located the remainder of the non-hydrogen atoms. All non-hydrogen atoms were refined with anisotropic displacement parameters. All hydrogen atoms were placed in ideal positions and refined as riding atoms with individual isotropic displacement parameters. The targeted complex was found, but it crystallized as two distinct isomers, labeled as primed and unprimed. Four nitrates (two 50% occupied) and one diethyl ether were located in addition to the two cluster dications. The enormous number of atoms forced us to create a "big" version of SHELXL-93 (3400 parameters) on the Cray-2 in order to complete full-matrix least-squares refinements. Several of the carbon atoms were found to be non-positive definite toward the end of the process and were restrained to be positive definite with the ISOR command. The nitrates were all restrained with common N−O bond lengths and idealized trigonal planar geometry. The isotropic displacement parameters of these nitrates are high, as expected. Tables 1−3 contain crystal and refinement information, selected atomic coordinates and equivalent isotropic displacement parameters, and selected distances and angles. Complete information is given in Tables S1−S4 as Supporting Information. Thermal ellipsoid representations of the cluster cores of both isomers are shown in Figures 4 and 5 and for the entire molecules in Figures S2 and S3 of the Supporting Information.

Acknowledgment. This work was supported by grants from the National Science Foundation (CHE-9222411) and the University of Minnesota Supercomputer Institute. We acknowledge Dr. Victor J. Young, Jr., and the University of Minnesota X-Ray Crystallographic Laboratory for the X-ray structural determination. We also thank professors Wilmer Miller and William B. Tolman for helpful discussions.

Supporting Information Available: Tables of data collection and refinement details, all atom parameters, bond lengths, bond angles, and anisotropic thermal parameters and thermal ellipsoid drawings of the complete molecule for **3**, a sample H_2-D_2 equilibration rate plot, and tables of kinetic data (36 pages). Ordering information is given on any current masthead page.

IC9515160

(26) SHELXTL-Plus V5.0, Siemens Industrial Automation, Inc., Madison, WI.